

Supporting Information

Multicomponent triformylphoroglucinol-based covalent organic framework for overall hydrogen peroxide photosynthesis

Erchong Chai,¹ Lanting Huang,¹ Lei Jiao,^{2,3} Zhiwei Xiao,² Xiang Zhang,^{*2,3,4} and Yaobing Wang^{*2,3,4}

¹ College of Chemistry, Fuzhou University, Fuzhou 350116, Fujian, P. R. China.

² CAS Key Laboratory of Design and Assembly of Functional Nanostructures, and Fujian Provincial Key Laboratory of Nanomaterials, State Key Laboratory of Structural Chemistry, Fujian Institute of Research on the Structure of Matter, Chinese Academy of Sciences, Fuzhou 350002, Fujian, P. R. China.

³ University of Chinese Academy of Sciences, Beijing 100049, P. R. China.

⁴ Fujian Science and Technology Innovation Laboratory for Optoelectronic Information of China, Fuzhou 350108, Fujian, P. R. China.

Email: zhangxiang@fjirsm.ac.cn; wangyb@fjirsm.ac.cn

Part Experimental Section. Materials. 2,2'-bipyridine-5,5'-diamine (Bpy, >97%) and 1,3,5-triformylphloroglucinol (Tfp, >97%) were from Shanghai Tensus Biotech Co., Ltd. N, N-dimethylacetamide (DMAC, 99.8%, Extra Day, with molecular sieves, water \leq 50 ppm) was provided by Energy Chemical. and 2,6-Diaminoanthraquinone (Daaq) were purchased from Aladdin.

Synthesis of COF-Tfp-BpyDaaq. 2.5 mmol (475.5 mg) of p-toluene sulphonic acid (monohydrate) was taken in a mortar followed by the addition of 0.225 mmol of corresponding diamine 2,2'-bipyridine-5,5'-diamine (Bpy) 53.6mg, 2,6-Diaminoanthraquinone (Daaq) 41.65 mg. The reaction mixture was thoroughly ground with a pestle for 5 minutes. Then 0.3 mmol (63 mg) of 1,3,5-triformylphloroglucinol (Tfp) was added to the mixture and mixing was continued for another 10 minutes until there is a certain color change. Then \sim 100 μ L (5.5 mmol) of water was added dropwise to the mixture and then the mixture was ground again for another 5 minutes. The amount of water varies for different COFs. The addition of water made a certain color change from pale to deep color. The mixture was transferred into a glass vial and heated for 60 seconds in an oven at 170 $^{\circ}$ C. It produced a deep reddish powder. The mixture was left for cooling to room temperature. The vial was then filled up with water for through washing off the excess PTSA. The powder was then treated several times with N,N-dimethylacetamide, water and acetone sequentially for the removal of residual molecular contaminants and dried under reduced pressure until further use (yield, 75%).

Synthesis of COF-Tfp-Bpy. 2.5 mmol (475.5 mg) of p-toluene sulphonic acid (monohydrate) was taken in a mortar followed by the addition of 0.45 mmol of corresponding diamine 2,2'-bipyridine-5,5'-diamine (Bpy) 83.8mg. The reaction mixture was thoroughly ground with a pestle for 5 minutes. Then 0.3 mmol (63 mg) of 1,3,5- triformylphloroglucinol (Tfp) was added to the mixture and mixing was continued for another 10 minutes until there is a certain color change. Then \sim 100 μ L (5.5 mmol) of water was added dropwise to the mixture and then the mixture was ground again for another 5 minutes. The amount of water varies for different COFs. The addition of water made a certain color change from pale to deep color. The mixture was transferred into a glass vial and heated for 60 seconds in an oven at 170 $^{\circ}$ C. It produced a deep reddish powder. The mixture was left for cooling to room temperature. The vial was then filled up with water for through washing off the excess PTSA. The powder was then treated several times with N,N-dimethylacetamide, water and acetone

sequentially for the removal of residual molecular contaminants and dried under reduced pressure until further use (yield, 72%).

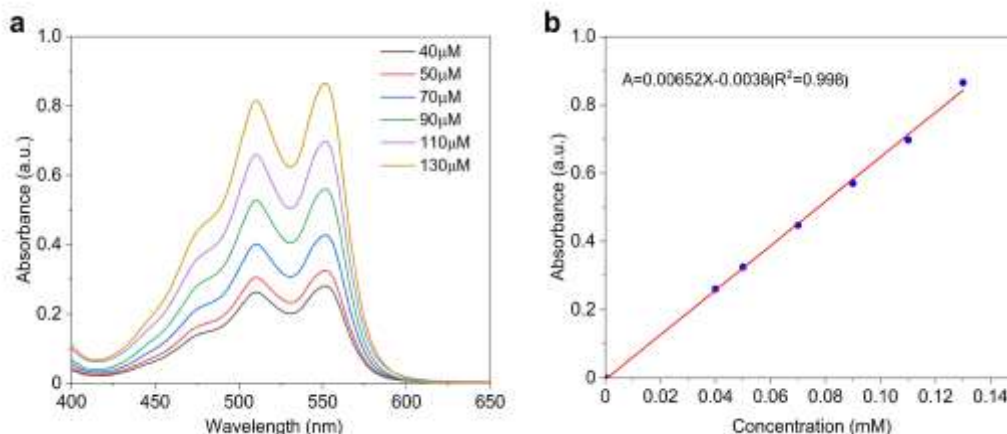
Synthesis of COF-Tfp-Daaq. 2.5 mmol (475.5 mg) of p-toluene sulphonic acid (monohydrate) was taken in a mortar followed by the addition of 0.45 mmol of corresponding diamine 2,6-Diaminoanthraquinone (Daaq) 83.3mg. The reaction mixture was thoroughly ground with a pestle for 5 minutes. Then 0.3 mmol (63 mg) of 1,3,5- triformylphloroglucinol (Tfp) was added to the mixture and mixing was continued for another 10 minutes until there is a certain color change. Then ~100 μ L (5.5 mmol) of water was added dropwise to the mixture and then the mixture was ground again for another 5 minutes. The amount of water varies for different COFs. The addition of water made a certain color change from pale to deep color. The mixture was transferred into a glass vial and heated for 60 seconds in an oven at 170 °C. It produced a deep reddish powder. The mixture was left for cooling to room temperature. The vial was then filled up with water for through washing off the excess PTSA. The powder was then treated several times with N,N-dimethylacetamide, water and acetone sequentially for the removal of residual molecular contaminants and dried under reduced pressure until further use (yield, 68%).

Characterization. The morphology of the photocatalysts was examined by scanning electron microscopy (SEM, JSM-7500) and transmission electron microscopy (TEM, 7650B, Hitachi). X-ray diffraction (XRD) patterns were obtained on a Netherlands 1710 diffractometer with Cu K α irradiation ($\lambda = 1.54 \text{ \AA}$). Fourier transform infrared spectroscopy (FTIR) spectra were recorded on a Bruker VERTEX 700 spectrometer. UV-vis diffuse reflectance spectra were recorded on a UV-2600 UV-VIS-NIR spectrometer (Shimadzu). BET specific surface area was determined by nitrogen adsorption-desorption isotherm measured at 77 K (NOVA 2200e). FTIR spectra were recorded on a Thermal-Nicolet 6700 spectrometer between 4000~500 cm^{-1} . Steady-state photoluminescence (PL) spectra were collected by a FluoroMax-4 spectrofluorometer (Horiba Scientific) and analysed with Origin-integrated software (FluoroEssencev2.2). Meanwhile, time-correlated single photon counting measurements were conducted using a single photon counting controller (Fluorohub, Horiba Scientific) to collect the photoluminescence decay profiles.

H₂O₂ photocatalysis. Photocatalytic H₂O₂ production. A flask was charged with the photocatalyst 5 mg, 20 mL H₂O, and sealed with a septum. The resulting suspension was ultrasonicated until the photocatalyst was dispersed before degassing thoroughly by O₂ bubbling for 20 min. And then, the mixture solution was stirred for 30 min under a dark condition to reach the absorption–desorption equilibrium. The reaction mixture was illuminated by a 10 W LED (PCX50C Discover, Beijing Perfectlight, China) and a 300 W Xe lamp (PLSSXE300D/300DUV, Beijing Perfectlight, China) with a 420 nm cutoff filter. All the reaction system was kept at 25 °C as controlled by cooling water.

H₂O₂ detection methods. Photocatalytic H₂O₂ production. A flask was charged with the photocatalyst 5 mg, 20 mL H₂O, and sealed with a septum. The resulting suspension was ultrasonicated until the photocatalyst was dispersed before degassing thoroughly by O₂ bubbling for 20 min. And then, the mixture solution was stirred for 30 min under a dark condition to reach the absorption–desorption equilibrium. The reaction mixture was illuminated by a 300 W Xe lamp (PLSSXE300D/300DUV, Beijing Perfectlight, China) with a 420 nm cutoff filter. All the reaction system was kept at 25 °C as controlled by cooling water.

H₂O₂ detection methods. DPD colorimetry was used to detect the concentration of H₂O₂: Sodium phosphate buffer was prepared by adding sodium dihydrogen phosphate (0.5 M) dropwise to the sodium dihydrogen phosphate solution (0.5 M) and testing the mixture until the pH equals 6. The 0.1 g of DPD was dissolved in 10 mL of 0.05 M H₂SO₄ solution. 5 mg of POD was dissolved in 5 mL of DI water. During the experiment, a 10 mL colorimetric tube was added 3 mL Sodium phosphate buffer, 1 mL sample aliquot was filtered by a 0.22 μM PES filter, 0.05 mL of DPD solution, 0.05 mL of POD solution, and 5.9 mL water. After the mixture was stirred for 50 s, the absorbance was measured at 551 nm by a UV/visible spectrophotometer (Agilent Technologies). The linear calibration curve of H₂O₂ concentration was obtained by diluting a 30% H₂O₂ stock solution to get the range of H₂O₂ concentration (50 ~ 200 μM). The linear relationship between H₂O₂ concentration and the absorption intensity was established as follows.



The apparent quantum yield (AQY) of photocatalyst was measured under 300W Xe lamp irradiation (equipped with band pass filter of 400 nm). The active area of reactor was approximately 4 cm². The monochromatic light intensity was averaged at 5 representative points with an optical power meter (Newport, model 1918-R). Therefore, the light intensity at 400 nm was calculated to be 8.95 mW cm⁻². Then, AQY was calculated by the following equation:

$$\text{AQY}(\%) = \frac{(\text{number of produced H}_2\text{O}_2 \text{ molecules}) \times 2}{\text{number of incident photons}} \times 100\%$$

Cycling Tests. After the reaction, the COFs-based photocatalyst was centrifuged, washed with methanol, and dried in a vacuum oven at 70 °C for 12 h. Then, the resulted photocatalyst was directly used for the subsequent runs.

Photocurrent measurement. The transient photocurrent response experiments were conducted on a CHI660D electrochemical system in a three-electrode system. The sample-coated fluoride-tin oxide (FTO) glass, Pt foil and Ag/AgCl electrode were used as the working electrode, counterelectrode and the reference electrode, respectively. 0.5 M Na₂SO₄ solution (evacuated with N₂) was utilized as the electrolyte.

In-situ DRIFTS measurement. In-situ diffuse reflectance infrared Fourier transform spectroscopy (DRIFTS) measurements were performed on a Bruker IFS 66v Fourier-transform spectrometer equipped with a Harrick diffuse reflectance accessory at the Infrared Spectroscopy and

Microspectroscopy Endstation (BL01B) in the National Synchrotron Radiation Laboratory (NSRL). Each spectrum was recorded by averaging 256 scans at a 2 cm⁻¹ spectral resolution. The samples were held in a custom-made IR reaction chamber, which was specifically designed to examine highly scattering powder samples in the diffuse reflection mode. The chamber was sealed with two ZnSe windows.

Rotating disk electrode (RDE) measurement. A glassy carbon rotating disk electrode (PINE Research Instrumentation, USA) was served as the substrate for working electrode. The working electrode was prepared as follows: 10 mg of the sample was dispersed in 2 mL of MeOH containing 20 μL of Nafion by ultrasonication. 10 μL of the above slurry was put onto the disk electrode and dried at room temperature. The linear sweep voltammogram (LSV) curves were recorded in an O₂-saturated 0.1 M phosphate buffer solution (pH = 7) at room temperature and a scan rate of 10 mV s⁻¹ with different rotation speeds. The average number of electrons (n) was calculated by the Koutecky-Levich equation:

$$\frac{1}{J} = \frac{1}{J_L} + \frac{1}{J_K} = \frac{1}{B\omega^{1/2}} + \frac{1}{J_K}$$
$$B = 0.62nFC_0D_0^{2/3}\nu^{-1/6}$$

where J is the measured current density, J_K and J_L are the kinetic and diffusion-limiting current densities, ω is the angular velocity, n is transferred electron number, F is Faraday constant (96485 C mol⁻¹), C₀ is the bulk concentration of O₂ (1.26 × 10⁻⁶ mol cm⁻³), D₀ is the diffusion coefficient of O₂ in 0.1 M phosphate buffer solution (2.7 × 10⁻⁵ cm² s⁻¹), and ν is the kinetic viscosity of the electrolyte (0.01 cm² s⁻¹).

Electron paramagnetic resonance (EPR) measurement. The EPR measurement was carried out on a spectrometer (Germany MS-5000) to detect oxygen-active species by adding 5,5-dimethyl-1-pyrroline N-oxide (DMPO) as a spintrapping reagent. The dispersion was purged with O₂ gas for 5 min before light irradiation. A Xe lamp (λ > 420 nm) was used as the light source.

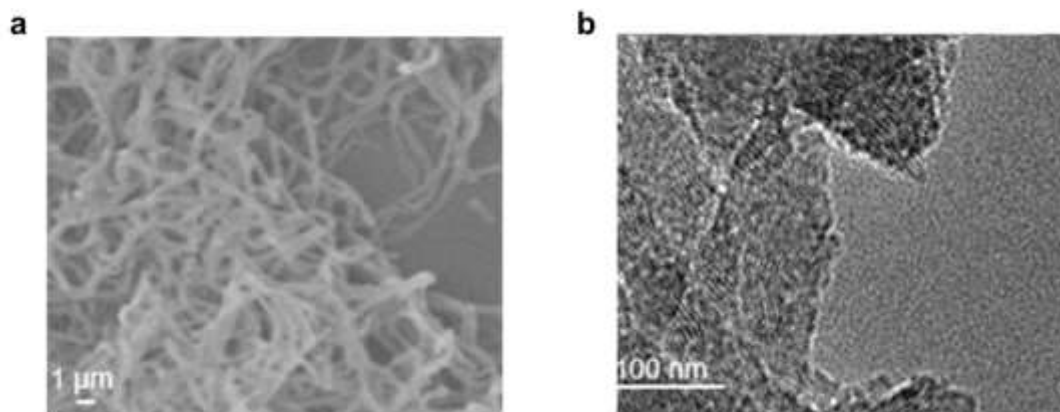


Figure S1. a) SEM images of COF-Tfp-BpyDaaq (b) TEM images of COF-Tfp-BpyDaaq.

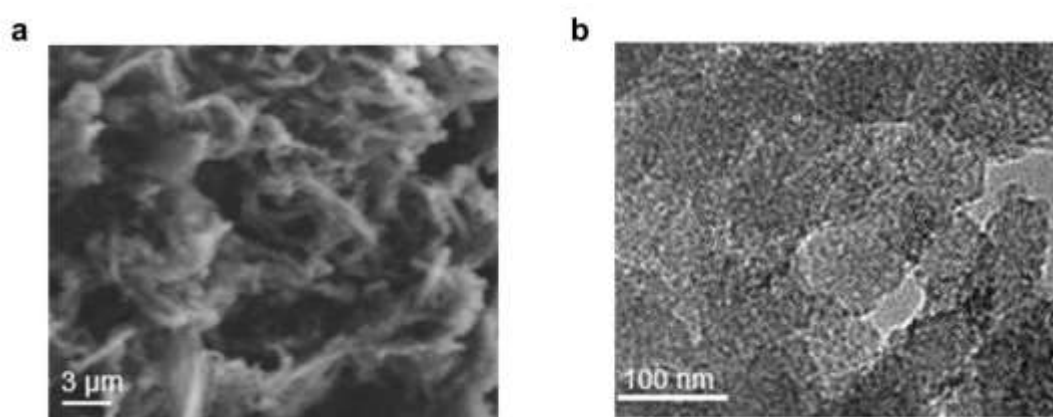


Fig. S2. a) SEM images of COF-Tfp-Bpy. (b) TEM images of COF-Tfp-Bpy.

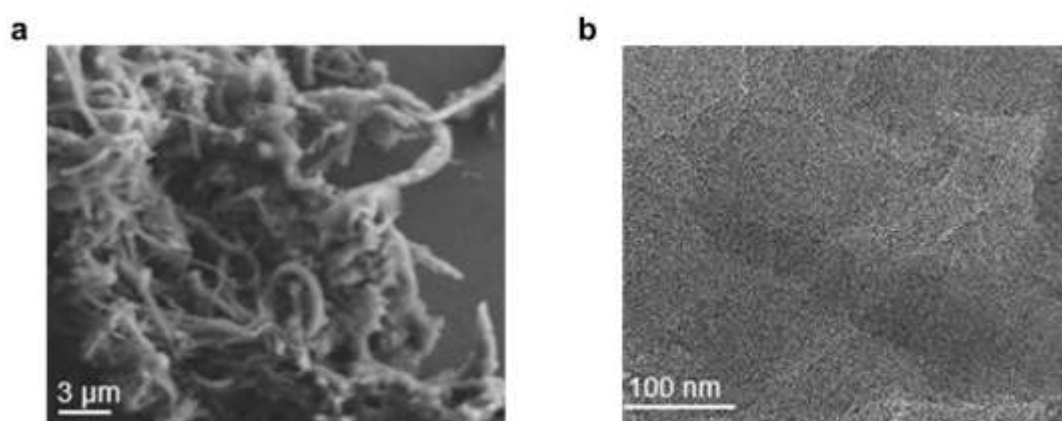


Fig. S3. a) SEM images of COF-Tfp-Daaq. (b) TEM images of COF-Tfp-Daaq.

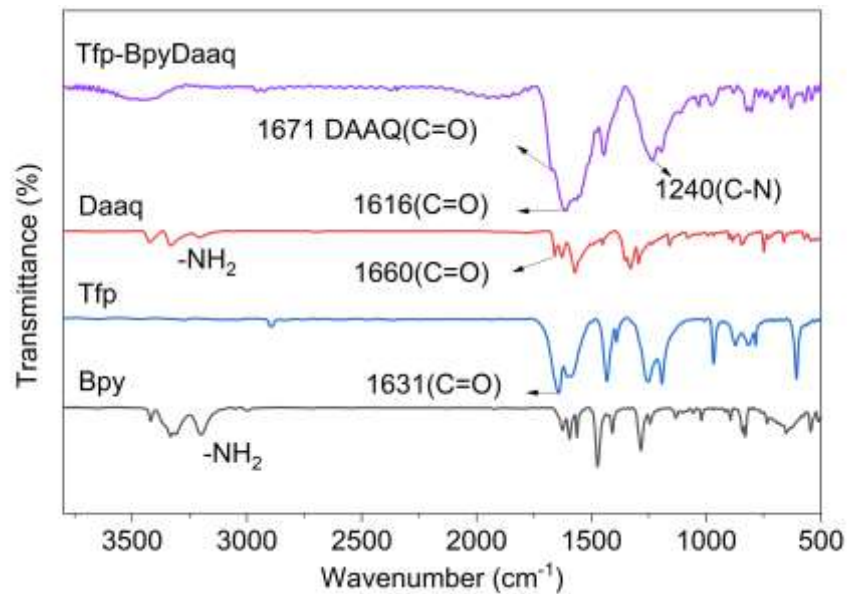


Fig. S4. FTIR spectra of Daaq, Tfp, Bpy and COF-Tfp-BpyDaaq.

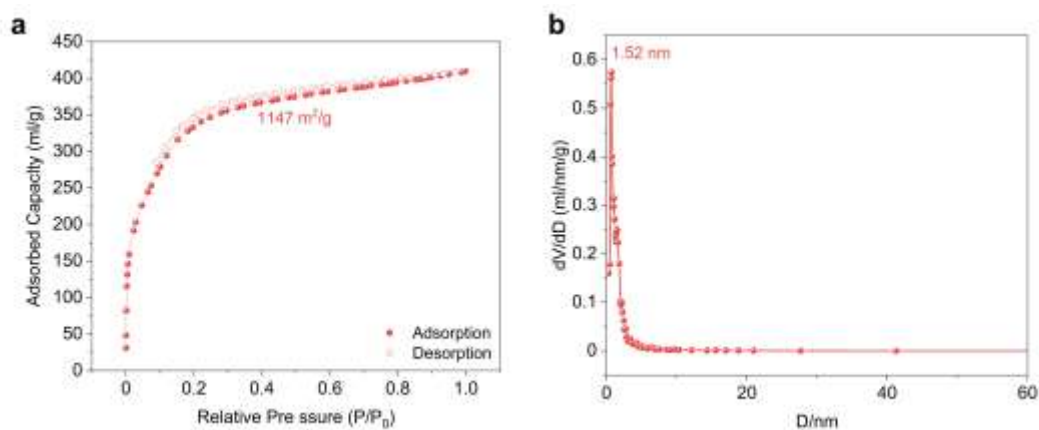


Fig. S5. Adsorption and desorption curve (a) and porosity data (b) of COF-Tfp-BpyDaaq.

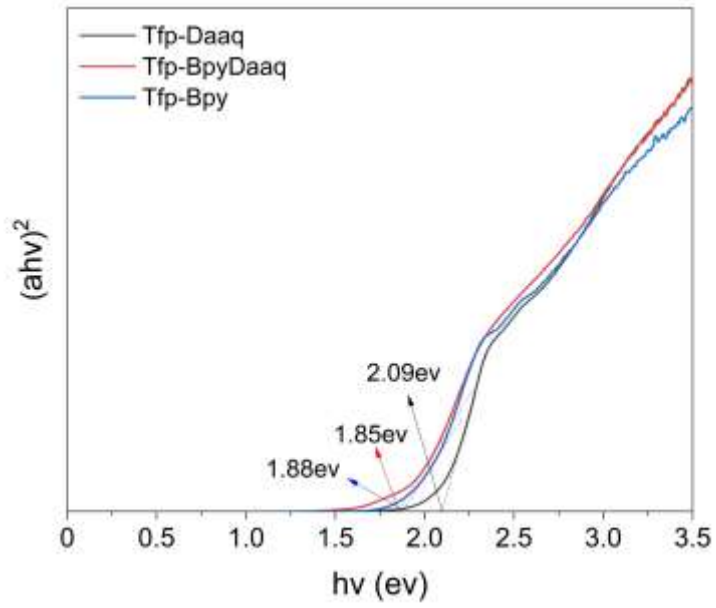


Fig. S6. Kubelka-Munk-transformed reflectance spectra of COFs.

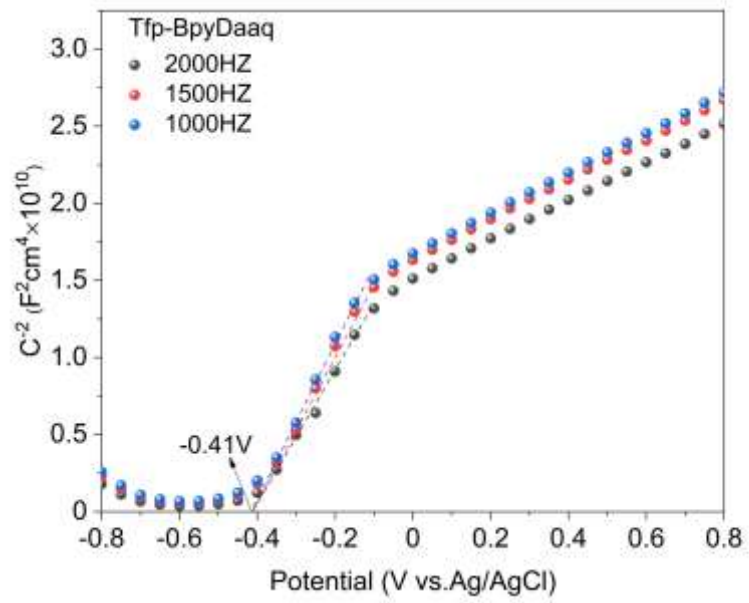


Fig. S7. Mott-Schottky plot of the COF-Tfp-BpyDaaq.

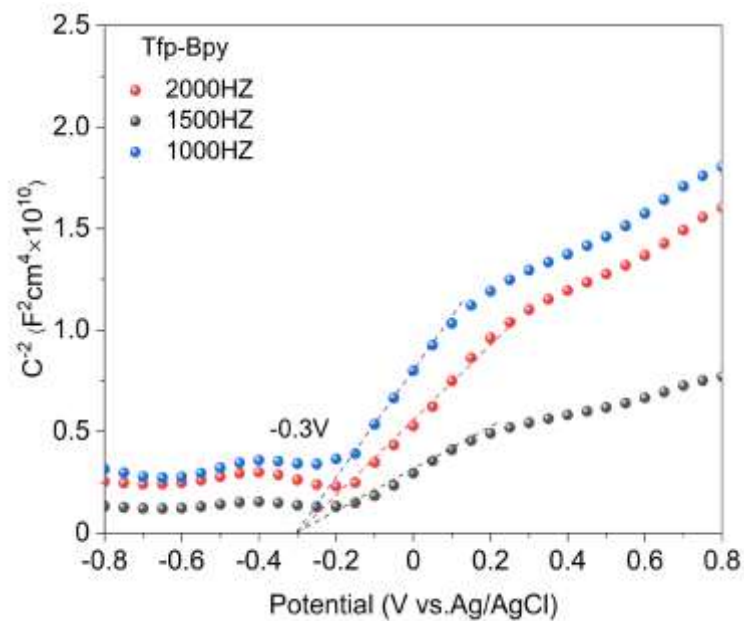


Fig. S8. Mott-Schottky plot of the COF-Tfp-Bpy.

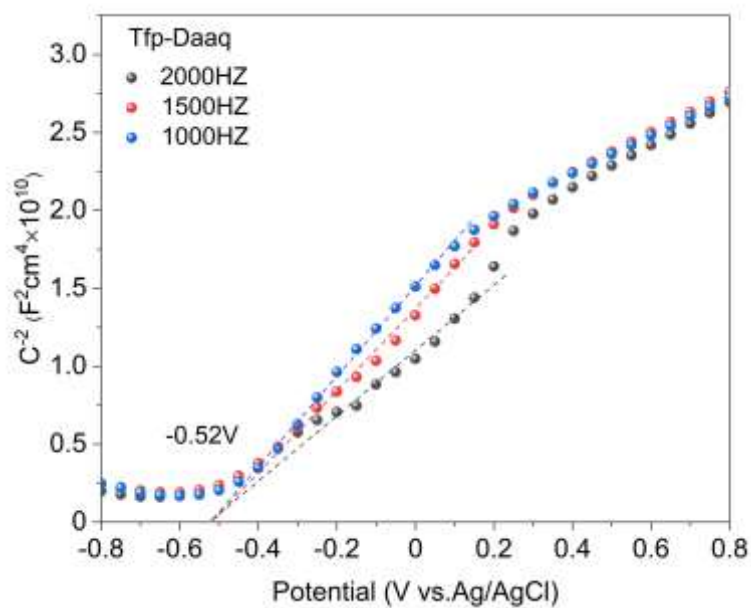


Fig. S9. Mott-Schottky plot of the COF-Tfp-Daaq.

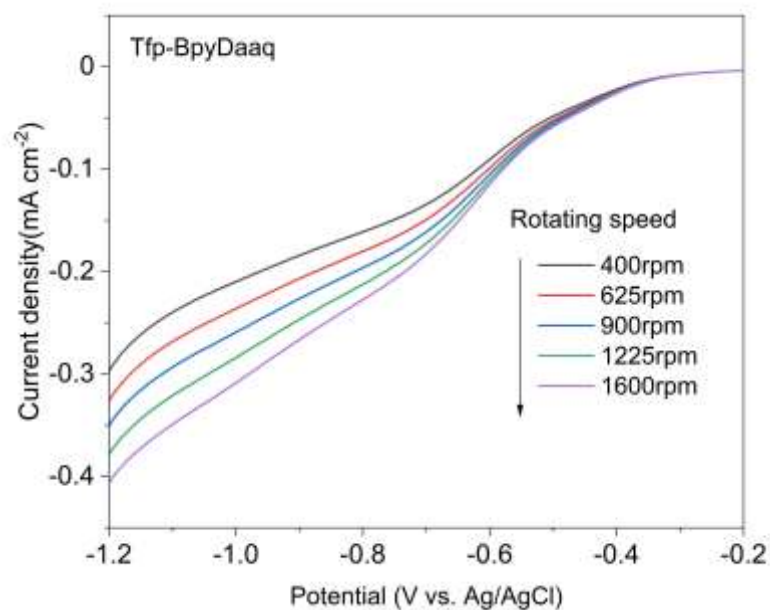


Fig. S10. Linear-sweep RDE voltammograms of COF-Tfp-BpyDaaq measured at different rotating speeds.

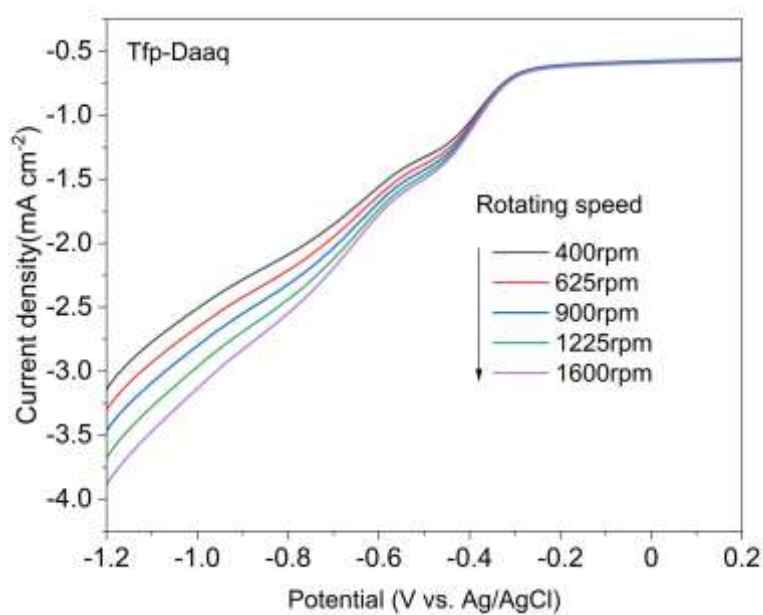


Fig. S11. Linear-sweep RDE voltammograms of COF-Tfp-Daaq measured at different rotating speeds.

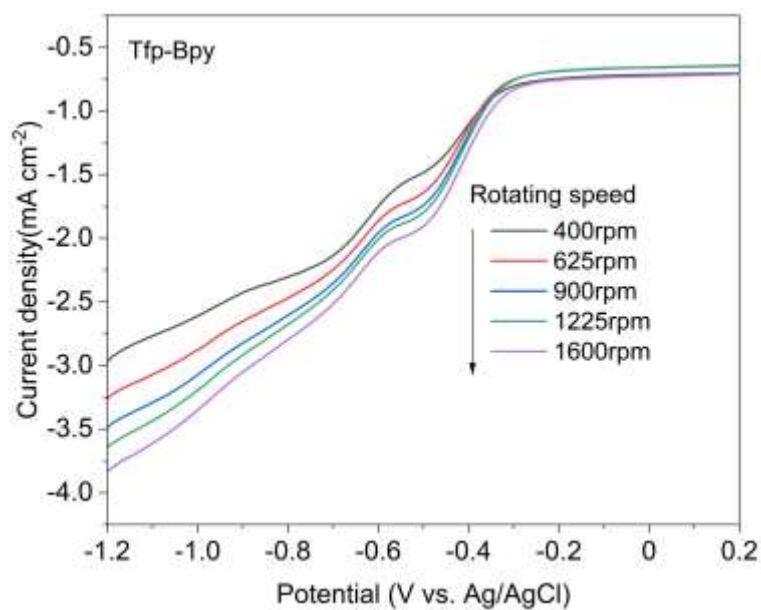


Fig. S12. Linear-sweep RDE voltammograms of COF-Tfp-Bpy measured at different rotating speeds.

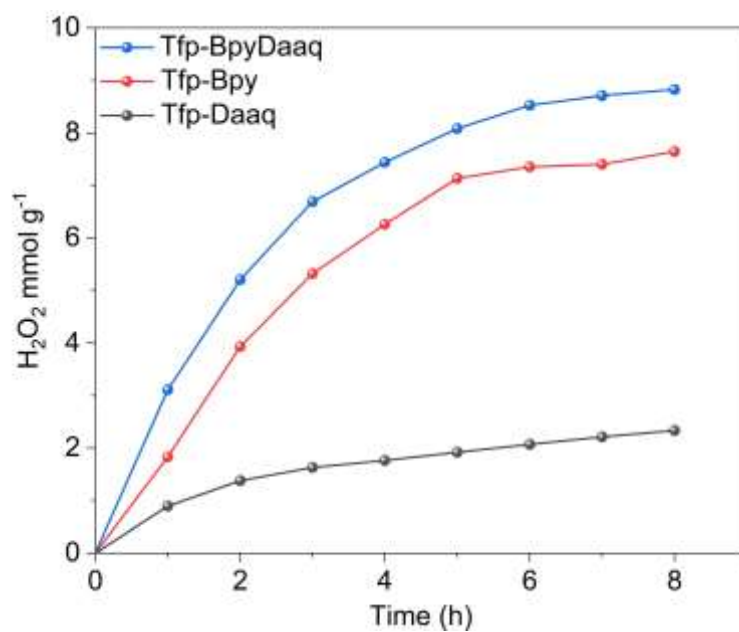


Fig. S13. Typical time course of photocatalytic production of H₂O₂ by as-synthesized COFs before exfoliation in O₂-saturated pure water under visible light irradiation.

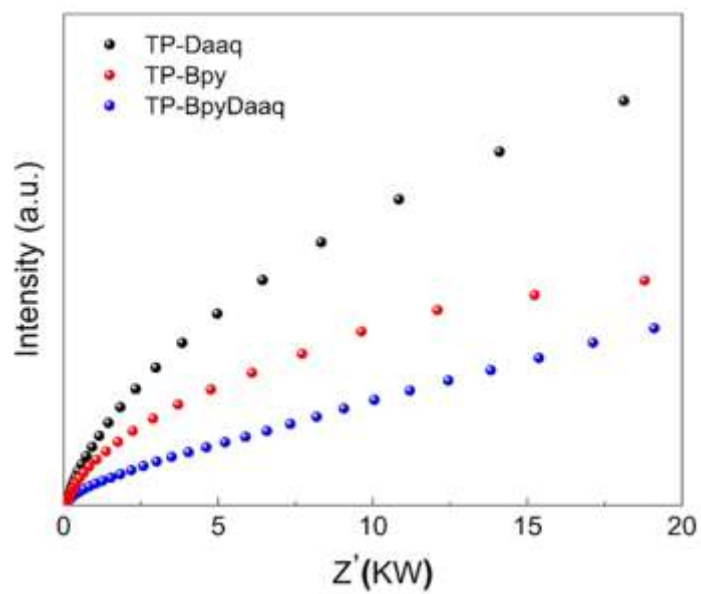


Fig. S14. PL spectra of COFs

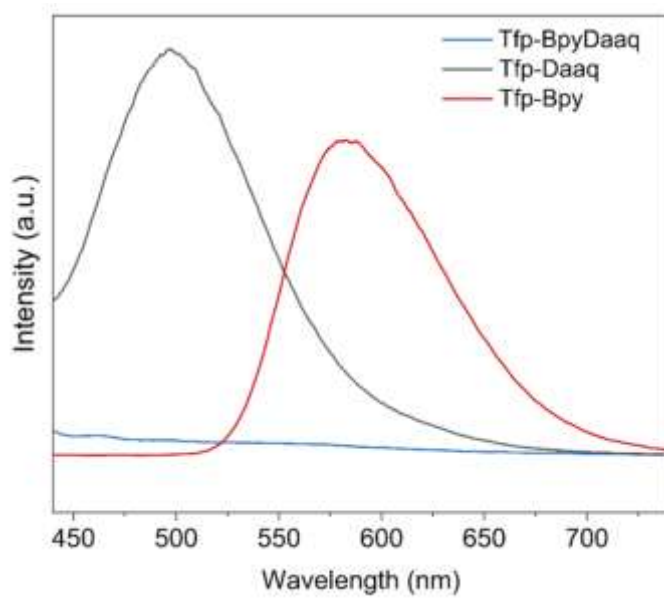


Fig. S15. Electrochemical impedance spectra of COFs

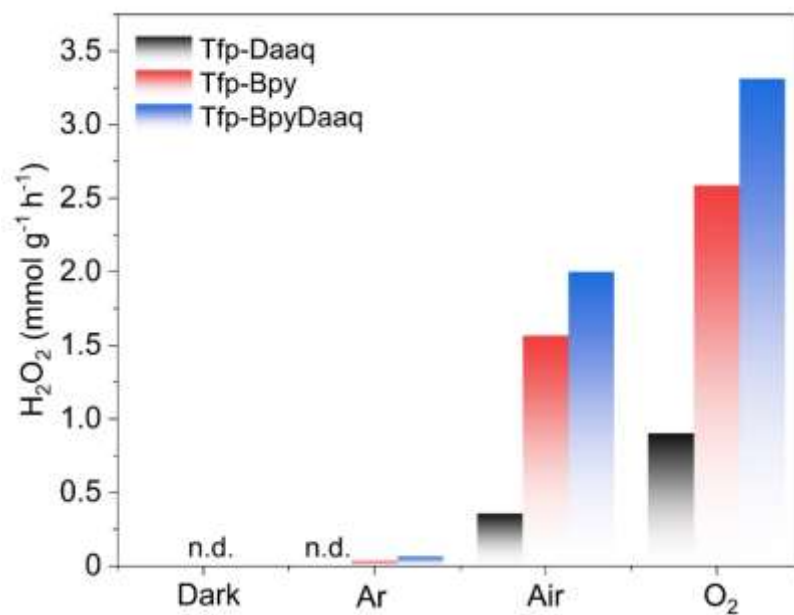


Fig. S16. Photochemical H₂O₂ production under different gas atmospheres.

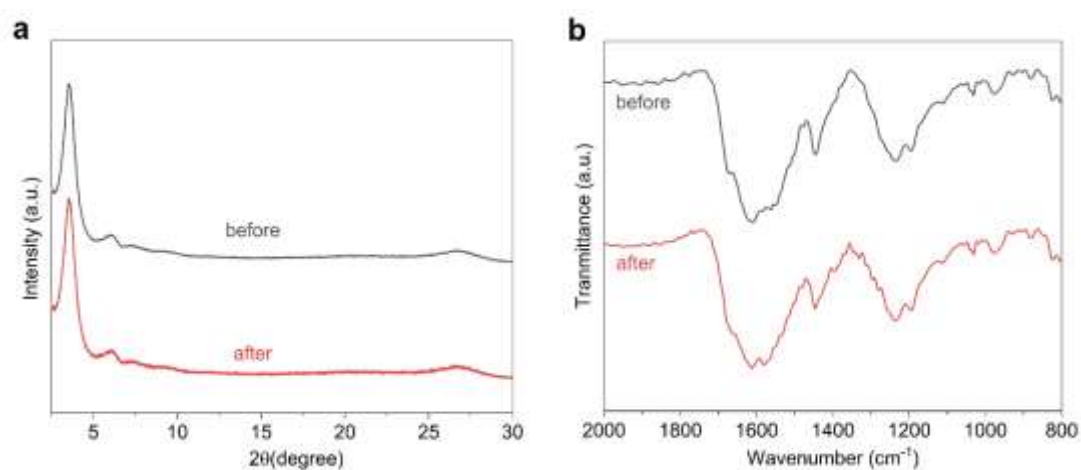


Fig. S17. (a) XRD of COF-Tfp-BpyDaaq before and after six cycles photocatalytic reaction. (b) IR of COF-Tfp-BpyDaaq before and after six cycles photocatalytic reaction.

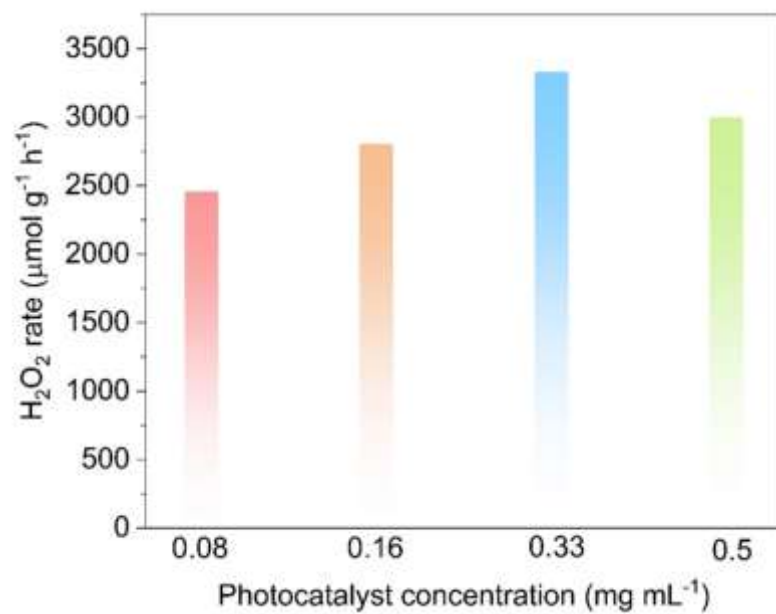


Fig. S18. Photocatalytic activity of COF-Tfp-BpyDaaq with different catalyst concentrations.

Table S1. The element of C, H, N and O for COF-Tfp-BpyDaaq, COF-Tfp-Daaq and COF-TfpBpy.

| Samples | | C (%) | H (%) | N (%) | O (%) |
|-------------|--------|-------|-------|-------|-------|
| Tfp-BpyDaaq | Calcd. | 68.9 | 3.07 | 11.39 | 16.64 |
| | Found | 67.3 | 3.67 | 10.31 | 15.89 |
| Tfp-Daaq | Calcd. | 69.79 | 2.91 | 7.07 | 20.23 |
| | Found | 69.9 | 3.79 | 7.63 | 19.88 |
| Tfp-Bpy | Calcd. | 66.38 | 3.61 | 16.16 | 13.85 |
| | Found | 65.97 | 4.27 | 14.95 | 14.41 |

Table S2. Performance of COF-Tfp-BpyDaaq for photocatalytic H₂O₂ generation compared with that of previously reported ternary photocatalysts Comparison of photocatalytic H₂O₂ generation performance.

| Photocatalysts | conditions | H ₂ O ₂ production rates | Reaction pathways | Refs |
|-----------------|--|--|--|---|
| COF-Tfp-BpyDaaq | O ₂ 0.33g/L, pure water; Xe-lamp AM 1.5G | 3332 μmol/g/h | Two-electron O ₂ reduction & two-electron water oxidization | This work |
| TTP | Air 0.2g/L, pure water Xe-lamp λ>420nm | 3132 μmol/g/h | Two-electron O ₂ reduction & four-electron water oxidization | Angew. Chem. Int. Ed. 2024, e202317214 (4 of 10) |
| DMCR-1NH | O ₂ 0.45g/L, water: IPA(10:1); Xe-lamp λ=420nm | 2588 μmol/g/h | Two-electron O ₂ reduction & two-electron alcohol to form an aldehyde | J. Am. Chem. Soc. 2023 , 145, 2975-2984. |
| RF-DHAQ | O ₂ 0.2g/L, pure water (10:1), Xe-lamp λ>420nm | 1820 μmol/g/h | Two-electron O ₂ reduction & two-electron water oxidization | Angew. Chem. Int. Ed. 2023, 62, e202218318 (4 of 6) |
| CTF-NS-5BT | O ₂ 0.45g/L, water: benzyl alcohol (9:1); Xe-lamp λ≥420nm | 1630 μmol/g/h | Two-electron O ₂ reduction & four-electron water oxidization | Adv. Sustainable Syst. 2021, 2100184 |